Short Broadband Fiber Gratings with Low Group Delay

Martin Becker, Ismael Chiamenti, Tino Elsmann, and Maria Chernysheva

***Abstract*—Fiber Bragg gratings (FBGs) are essential optical components, which due to their design flexibility offer numerous prospects for a wide range of applications in fiber laser, sensor, and telecommunication technologies. Here we demonstrate that a phase mask interferometer driven by a deep-ultraviolet femtosecond laser enables inscription of FBGs with top-hat spectral reflection bandwidth. FBGs with the bandwidth of 2 nm have been achieved with inscription of several superimposed narrow FBGs with bandwidth less than 0.2 nm. The induced refractive index modulation profile of the superimposed gratings has been investigated with two measurement methods, namely, optical frequency domain reflectometry and the layer-peeling method. The analysis has shown that the spatial modulation index profile follows a sinc profile and has a very narrow central peak of less than 0.4 mm. Importantly, the FBGs provide low group delay values in comparison to their chirped counterparts. Additionally, the small center structure makes such gratings ideal for fiber sensing with high local resolution. The demonstrated FBG inscription method, developed initially to fabricate optical reflectors for infrared laser systems, can be translated to other applications, such as biophotonics, telecommunications, sensing and astrophysics.**

***Index Terms*—Bragg filter, optical fiber filters, two-beam interferometry, femtosecond laser**

I. Introduction

BROADBAND FILTERS IN OPTICAL FIBERS have widespread applications in telecommunications, sensing, laser applications, in multi-core fiber devices and are an important element in spectroscopic applications, e.g. in life sciences and astronomy for the suppression of atmospheric fingerprints in the infrared wavelength region [1]. In telecommunications, broad reflection filters are desired for channel filtering, where particular dispersion properties are also desired to mitigate broadening of the pulse [2].

In fiber lasers, broadband reflecting fiber filters are required, naturally, to maintain wavelength matching during laser operation and achievement of highly-customised generation regimes, such as operation at ultrahigh repetition rates [3] or square-pulse generation [4], [5]. Furthermore, they can suppress self-mode-locking in continuous-wave lasers [6] and eliminate nonlinear effects, as stimulated-Raman-scattering [7]. Another splendid example of the application of broadband fibre filters in laser physics is the realisation of dispersive Fourier transform for single-shot spectral characterisation [8].

Typically, fibre Bragg gratings (FBGs) present the most compact, robust and flexible solution for the in-fibre filters, which bandwidth can be tailored by optimization of their fabrication method. Femtosecond laser inscription is proven approach to produce FBGs into a broad range of various types of fibers, including non-photosensitive fibers [9], [10]. Several methods for broadband FBG inscription with femtosecond lasers have been presented. Most of them target chirped Bragg grating structures fabrication. The most straightforward approach is the direct phase mask inscription with a chirped phase mask, which allows fabrication of chirped fiber Bragg gratings [11], [12]. Another phase mask approach uses a homogeneous phase mask to write short gratings exploiting the transverse walk off effect [13]. These methods require a well-tailored phase mask for every specific operational wavelength. The phase mask is located in close proximity to the

The authors are with the Leibniz Institute of Photonic Technology, Albert-Einstein-Strasse 9, 07745 Jena, Germany. e-mail: martin.becker@leibniz-ipht.de

I. Chiamenti is also with the Federal University of Technology - Paraná - UTFPR/DAELT, Av. Sete de Setembro 3165, 80230-901 Curitiba, Brazil

fiber during the inscription process, which might damage the phase mask during inscription due to strong focusing closely behind the phase mask. Secondly, the inscription with phase mask interferometer with non-homogeneous phase mask [14] allows flexible FBG inscription within a particular wavelength region. Alternatively, FBG inscription can be done by using a homogeneous phase mask and distorted wavefronts [15], [16]. Here one has to take care to achieve homogeneous illumination conditions over the grating length. The long-term inscription presents one of the solutions to enhance the photoinduced refractive index modulation and, therefore, expand the FBG bandwidth [17]. In practice, the grating bandwidth is limited due to non-linear glass photosensitivity and experimental conditions like beam point stability or coherence properties [18], [19]. Lastly, the point-by-point (plane-by-plane or line-by-line) inscription allows fabricating chirped FBGs with flexible parameters [20]. The main disadvantage of this method is that it requires advanced positioning systems to avoid stitching errors.

Here we present an inscription method to achieve broadband reflection filters in single-mode fibers in the telecom C-band, which uses a phase mask interferometer with a homogeneous phase mask and deep-UV femtosecond laser [21], [22]. We increased the spectral bandwidth of the resulting gratings through the fabrication of series of superimposed Bragg gratings [23]. The proposed methodology yielded in the development of FBGs with top-hat profile, short effective grating length, and low dispersion profile. This method has the potential to become an essential building block for further translation of FBG technology to special optical fibers, including rare-earth-doped silica fibers [24], phosphate, polymer and other fibers. The phase mask interferometer also allows expanding the presented inscription method to particular target wavelengths within the range from visible to infrared.

II. Superimposed FBG inscription

FBG inscription has been performed using a motorized phase mask interferometer (Fig. 1) and a frequency tripled femtosecond laser setup (Coherent Mantis with Legend Elite as an amplifier and a tripler unit) operated in ultraviolet output

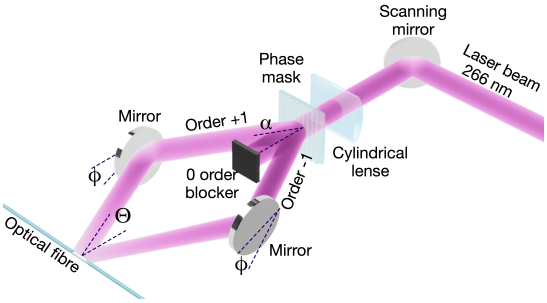

Fig. 1. Sketch of the phase mask interferometer

wavelength at 266 nm. Due to the short pulses of the laser system, we focused on symmetry of the inscription setup so that two rays corresponding to the first diffraction orders departing at phase mask position from the optical axis of the interferometer arrive at the position of the fiber without optical path length difference. The FBG central wavelength of the interferometer λ_{c} is defined by the period of the beam splitting phase mask Λ_{PM} (1075 nm, from Ibsen Photonics), and the effective mode field index n_{eff} as $\lambda_{\mathrm{c}} = n_{\mathrm{eff}}\Lambda_{\mathrm{PM}}$. The tuning range is limited by the temporal coherence properties of the inscription laser [21], [14]. Thus, the interferometer used in our experiments allows a FBG wavelength span of several tens of nanometers for the applied laser system. In our experiments, the target FBG parameters were as following: central reflection wavelength of 1555 nm, the reflection bandwidth 2 nm (top hat profile), and the reflection intensity of 50%. These parameters were chosen to fit the requirements for a distributed back reflector fiber laser. The gratings under tests were inscribed in standard single-mode fibers (ITU-T G652).

The Bragg wavelength inscribed with the phase mask interferometer (Fig. 1) is determined by the following equation:

$$\lambda_{\mathrm{Bragg}} = \frac{n_{\mathrm{eff}}\lambda_{\mathrm{inscr}}}{\sin\left(2\phi + \alpha\right)} \quad , \tag{1}$$

here λ_{inscr} is the inscription wavelength, α is the diffraction angle behind the beam splitter ($\sin\alpha = {}^{\lambda_{\mathrm{inscr}}}/_{\Lambda_{\mathrm{PM}}}$), and ϕ is the rotation angle of the mirrors compared to the parallel position (see Fig. 1).

The FBGs were inscribed in a recursive procedure starting with the determination of broadband FBG reflection intensity target, 50% in our case. Additionally, we put a lower limit, between 10% and 20% of the target value. Gratings below the limit are considered as valleys. The starting angular position of the interferometer mirrors ϕ was determined via equation 1 according to the desired 1554 nm Bragg wavelength, corresponding to blue edge of broadband FBG reflection spectrum. After that, a standard narrowband FBG is produced. The reflection spectrum of the grating is constantly monitored during the inscription process of the gratings. When the reflection intensity reaches a target value the inscription process is stopped and the next step is started, assisted by the monitoring of the intensity reflection until it reaches the chosen target value. Once the inscription is done, the femtosecond laser beam is blocked, and the mirrors are rotated with an angular shift of $\phi = 0.0011°$, representing a Bragg wavelength shift of $\sim$0.22 nm). A new narrowband FBG is inscribed, also assisted by the monitoring of the intensity reflection.

Fig. 2 presents the reflection broadening of the FBG during the inscription. There were 10 superimposed FBGs, spectrally separated by $\approx$0.22 nm. A positive wavelength shift of the superimposed fiber Bragg gratings reflection is observed during inscription, which shifts to longer wavelengths. Such behavior is attributed to the change of the effective index of refraction, as proposed by *Othonos et al.* [23]. It is possible to identify the formation of two valleys in the FBG spectrum with the final position at 1555 and 1555.6 nm, after the 6^{th} and 9^{th} FBGs, correspondingly.

To mitigate formation of the valleys and achieve the flat top-hat spectral profile, the inscription procedure was optimized. The reflection spectrum intensity was carefully controlled after inscription of each grating. If a valley is formed between the peak reflection of two consecutive FBGs, the laser is blocked, and the mirrors are rotated back at the half value of the previous rotation step (to the middle between the previous and the new positions). Then a new FBG is inscribed until the chosen target value is reached. If the intensity of the previous FBG is reduced then the mirrors are rotated back to its related angular position, repeating the inscription until the reflection target is reached again.

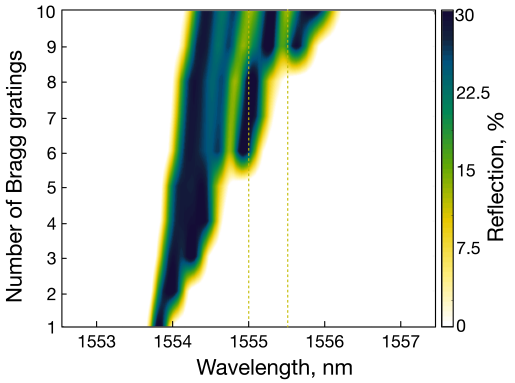

Fig. 2. Reflection evolution during the superimposed FBG inscription

III. FBG CHARACTERISATION AND RESULTS

Fig. 3 shows the reflection spectrum of FBG inscribed by an optimized procedure, fulfilling all set requirements of the top-hat profile ($\approx$2 nm bandwidth, $\approx$50% reflectivity). The corresponding group delay shows small ripples $\pm$6 ps at the center of the spectrum. Such fluctuations correspond to a variation of the reproach plane (effective reflection position) of $\pm$600 μm inside of the Bragg reflection band.

A series of broadband FBGs has been inscribed with similar reflectivity, Bragg wavelength, and bandwidth. Table I summarises the bandwidth of four FBGs, showing good repeatability of the experimental results.

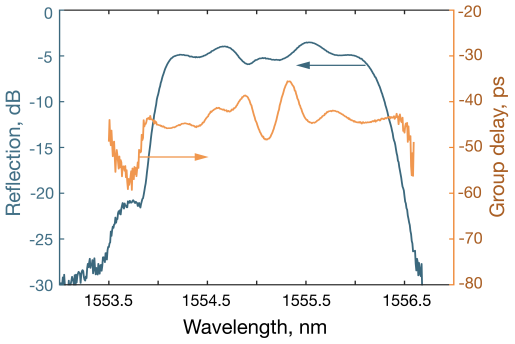

Fig. 3. Reflection and group delay of grating number 1

The investigation of the index profile distribution of the superimposed grating structures requires the measurement of the complex reflection spectrum of the FBGs. To obtain parameters of the grating profile, we used Optical Frequency Domain Reflectometry (OFDR, RTS150 from 4DSP LLC). The measurement system comprises a tunable laser system and a broadband fiber optic mirror (Thorlabs) as a reference. The mirror and the FBG form a Fabry-Pérot device, which is measured in reflection. The modulation profile is then derived by fast Fourier transformation of the signal train measured during a single sweep. The spatial resolution of the measurement system can be estimated from the sampling depth of the wavelength measurement (20 bit) and the wavelength span (18 nm in the telecom C-band). The resolution is around 46 µm.

As a control reference, we applied the layer peeling method, performed according to the procedure described in [25]. To achieve the required complex reflectivity, we used differential phase shift measurement to obtain the reflection spectrum and the group delay simultaneously. The measurement system is based on an optical network analyzer (OptScope Q7750 from Advantest): a tunable modulated laser source (modulation speed 3 GHz) together with a light phase comparator. One measurement of a broad band grating is shown in Fig. 3.

For layer peeling, the spatial grating distribution is discretized into a sequence of alternating reflection and transmission layers, each one is defined by a 2×2 matrix containing the local reflection and phase transition respectively. The starting reflectivity ρ_1 can be found by the numerical averaging of the measured complex reflectivities $r_1(m)$ of superimposed FBGs, which includes information on their phase, as:

$$\rho_1 = \frac{1}{M}\sum_{m=1}^{M} r_1(m) \quad , \tag{2}$$

here M is the number of data points of the discretized spectrum.

For the first layer outside of the grating the reflected phase of the discretized reflection values appears to be randomized, which leads equation 2 to be zero for the first element. Afterwards, the adjacent transmission layer is characterized by the phase transition through the grating element, the layer can be 'peeled' off, and the next layer can be determined. As the calculation proceeds through the layers and the numerical position approaches the grating, the phase values of the discretized reflection values approximate and equation 2 gives non-zero results.

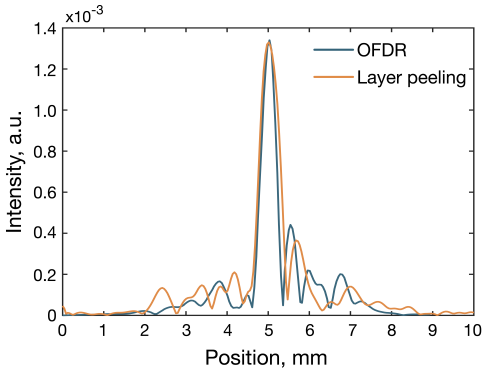

Fig. 4. Reconstructed index modulation profile of grating number 1

The results of the OFDR measurement system and the layer peeling method for the grating with the spectral profile presented in Fig. 3 can be found in Fig. 4. Both methods indicate a local modulation profile with a short sharp central peak <0.4 mm and low-intensity side lobes.

IV. Discussion

The grating reflection profile and the refractive index modulation are related by the Fourier transform for weak gratings [26], hence one might expect that through the application of superimposed gratings it should be possible to generate broadband reflection filters with low variation of dispersion. Assuming that the symmetry of the interferometer causes symmetry of the FBG index modulation profile it is considered, that the sinc function is to be a theoretical basis to explain the top-hat Bragg reflection spectra [27], [28]. In this case, one can calculate the period of the modulation index profile Δz from the top-hat reflection profile $\Delta\lambda_{\mathrm{Bragg}}$ via Fourier transform through the relation

$$\Delta z = \frac{\lambda_{\mathrm{Bragg}}^2}{2n_{\mathrm{eff}}\Delta\lambda_{\mathrm{Bragg}}} \quad . \tag{3}$$

TABLE I
FBG PROFILE PERIODS AND SPECTRAL BANDWIDTHS TOGETHER WITH CALCULATED VALUES

FBG	spectral width		peak width	
	measured	estimated	measured	estimated
1	2.2 nm	2.3 nm	370 µm	387 µm
2	2.2 nm	2.3 nm	360 µm	380 µm
3	2.4 nm	2.4 nm	353 µm	348 µm
4	2.2 nm	2.3 nm	367 µm	381 µm

TABLE II
THEORETICAL REFLECTIVITY, BANDWIDTH (BW), GROUP DELAY VARIATION (GDLV) AND GDL-RIPPLES OF BROADBAND GRATING TYPES

Type	Refl.	BW	GDLV	Ripples
rect.	100%	1.4 nm	≈ 10 ps	none
chirp	100%	3.3 nm	100ps	40 ps
sinc	40%	2.3 nm	none	0.6 ps

To confirm that Eq. 3 is related to a series of superimposed Bragg gratings, one can assume that the superimposed grating structure comprises a number of slightly different Bragg grating periods with spacing $\Delta\lambda_{step}$. The superimposed grating profile can be derived in a similar way to the theory of multiple slit interference, with the refractive index modulation of the grating expressed by

$$\Delta n_{\mathrm{mod}}(z) = \Delta n_{\mathrm{mod}}(0)\frac{\sin\left(\frac{1}{2}N\Delta kz\right)}{\sin\left(\frac{1}{2}\Delta kz\right)}\cdot p(z) \quad , \tag{4}$$

where $p(z)$ is the modulation envelope induced by the laser beam profile with the center at the optical axis of the interferometer (z=0). N is the number of gratings and Δk is the wavenumber spacing, here approximated by $\Delta k \approx -2\pi n_{\mathrm{eff}}\Delta\lambda_{step}/\lambda^2_{\mathrm{Bragg}}$. Looking for the zeros of Eq. 4 one gets directly Eq. 3.

Table I summarises the spectral bandwidth and the width (minima spacing) of the grating reflection profile peak along the length of the series of developed superimposed FBGs. The spectral width is taken from the reflection spectra measurements and the width of the grating reflection profile peak is taken from the OFDR measurement and layer peeling. Both measurements are put in correlation through equation 3, which describes the minimal spacing of a sinc-shaped profile. Assuming an uncertainty of 0.1 nm and 46 µm, the results from the layer peeling and the OFDR measurement are mutually in good agreement. Measurement uncertainties arise due to measurement noise of the OFDR measurement system and the network analyzer as well as non-perfect side slopes of the gratings.

Conventionally, to achieve a broadband reflection, chirped-FBGs [14] or short homogeneous FBGs [29] are applied. In Table II we compared the types of gratings with 1 cm in length and index modulation amplitude of $\Delta n_{\mathrm{mod}} = 1\times10^{-3}$ with the transfer matrix method [30]. The chirped grating has a chirp of 2.3 nm/cm and the sinc grating has a period similar to Table I. The group delay variation inside of the reflection band is linear for the chirped grating and depends on the grating length, it is U-shaped for the long exposure grating and there is almost no dispersion for the sinc grating.

According to the fiber Bragg grating length there is no direct physical limit, but in comparison with standard FBGs, the length of the peak of the index modulation and the spectral width are correlated. Using a value for the index modulation of $\Delta n_{\mathrm{mod}} = 1 \times 10^{-3}$ we get reflectivities from 45% (2 nm bandwidth) down to 5% (7 nm bandwidth).

In these regards, the presented superimposed FBGs ensure both benefits of a spectral top-hat reflection and quasi-constant group delay due to their short-length with sinc refractive index profile. Such short gratings are useful for fiber sensing with high local resolution [29], [13].

V. SUMMARY AND OUTLOOK

We have shown the inscription of superimposed FBGs with a phase-mask interferometer and UV femtosecond laser to achieve broadband reflection. The suggested recursive methodology allows achieving the desired bandwidth and top-hat profile eliminating the risk of valleys formation in the reflection spectrum. The top-hat reflection spectrum profile with the bandwidth over 2 nm, as well as a short <0.4 mm length of the resulting FBGs, have been confirmed by OFDR and layer-peeling approach, assisted with optical network analyzer measurements. Remarkably, the inscribed FBG demonstrate quasi-constant group delay with a negligible ripple of ±6 ps, which can be further decreased by improving the stability of

the inscription setup (e.g. motor accuracy, beam point stability). We believe that the demonstrated approach paves the way to the development of a new generation of advanced broadband fiber Bragg gratings for applications in laser technology as well as strain and temperature sensing with enhanced local resolution.

ACKNOWLEDGEMENTS

Co-funding by the ERDF program and by the Thuringian Ministry of Education, Science and Culture is gratefully acknowledged.

REFERENCES

[1] J. Bland-Hawthorn, S. C. Ellis, S. G. Leon-Saval, R. Haynes, M. M. Roth, H. G. Löhmannsröben, A. J. Horton, J. G. Cuby, T. A. Birks, J. S. Lawrence, P. Gillingham, S. D. Ryder, and C. Trinh, "A complex multi-notch astronomical filter to suppress the bright infrared sky," *Nature Commun.*, vol. 2, no. 1, pp. 1–7, 2011.

[2] F. Knappe, H. Renner, and E. Brinkmeyer, "Efficient design of spatially symmetric Bragg gratings for add/drop multiplexers," *AEU - International Journal of Electronics and Communications*, vol. 62, no. 7, pp. 513–520, 2008.

[3] J. Azaña, R. Slavík, P. Kockaert, L. R. Chen, and S. LaRochelle, "Generation of customized ultrahigh repetition rate pulse sequences using superimposed fiber Bragg gratings," *J. Lightw. Technol.*, vol. 21, no. 6, p. 1490, 2003.

[4] M. Marano, S. Longhi, P. Laporta, M. Belmonte, and B. Agogliati, "All-optical square-pulse generation and multiplication at 1.5 μm by use of a novel class of fiber Bragg gratings," *Opt. Lett.*, vol. 26, no. 20, pp. 1615–1617, 2001.

[5] I. Kudelin and M. Chernysheva, "Square pulse and harmonic ultrashort pulse generation in semiconductor optical amplifier-based Mamyshev oscillator," in *2019 Conference on Lasers and Electro-Optics Europe & European Quantum Electronics Conference (CLEO/Europe-EQEC)*. IEEE, 2019, pp. 1–1.

[6] H. Xu, M. Jiang, P. Zhou, G. Zhao, and X. Gu, "Elimination of self-mode-locking pulses in high-power continuous-wave Yb-doped fiber lasers with external feedback," *Appl. Opt.*, vol. 56, no. 32, pp. 9079–9083, 2017.

[7] H. Xu, M. Jiang, C. Shi, P. Zhou, G. Zhao, and X. Gu, "Spectral shaping for suppressing stimulated-Raman-scattering in a fiber laser," *Appl. Opt.*, vol. 56, no. 12, pp. 3538–3542, 2017.

[8] S. Hamdi, A. Coillet, and P. Grelu, "Real-time characterization of optical soliton molecule dynamics in an ultrafast thulium fiber laser," *Opt. Lett.*, vol. 43, no. 20, pp. 4965–4968, 2018.

[9] D. Grobnic, S. J. Mihailov, R. B. Walker, C. W. Smelser, C. Lafond, and A. Croteau, "Bragg gratings made with a femtosecond laser in heavily doped Er-Yb phosphate glass fiber," *IEEE Photon. Technol. Lett.*, vol. 19, no. 12, pp. 943–945, 2007.

[10] S. J. Mihailov, D. Grobnic, C. W. Smelser, P. Lu, R. B. Walker, and H. Ding, "Bragg grating inscription in various optical fibers with femtosecond infrared lasers and a phase mask," *Opt. Mat. Express*, vol. 1, no. 4, p. 754, 2011.

[11] M. Bernier, D. Faucher, R. Vallée, A. Saliminia, G. Androz, Y. Sheng, and S. L. Chin, "Bragg gratings photoinduced in ZBLAN fibers by femtosecond pulses at 800 nm," *Opt. Lett.*, vol. 32, no. 5, pp. 454–456, 2007.

[12] M. Bernier, D. Faucher, N. Caron, and R. Vallée, "Highly stable and efficient erbium-doped 28 µm all fiber laser," *Opt. Express*, vol. 17, no. 19, p. 16941, 2009.

[13] C. Hnatovsky, D. Grobnic, and S. J. Mihailov, "Through-the-coating femtosecond laser inscription of very short fiber Bragg gratings for acoustic and high temperature sensing applications," *Opt. Express*, vol. 25, no. 21, p. 25435, oct 2017.

[14] M. Becker, T. Elsmann, I. Latka, M. Rothhardt, and H. Bartelt, "Chirped phase mask interferometer for fiber Bragg grating array inscription," *J. Lightw. Technol.*, vol. 33, no. 10, 2015.

[15] J. Thomas, C. Voigtländer, D. Schimpf, F. Stutzki, E. Wikszak, J. Limpert, S. Nolte, and A. Tünnermann, "Continuously chirped fiber Bragg gratings by femtosecond laser structuring," *Opt. Lett.*, vol. 33, no. 14, p. 1560, 2008.

[16] C. Voigtländer, R. G. Becker, J. Thomas, D. Richter, A. Singh, A. Tünnermann, and S. Nolte, "Ultrashort pulse inscription of tailored fiber Bragg gratings with a phase mask and a deformed wavefront," *Opt. Materials Express*, vol. 1, no. 4, p. 633, aug 2011.

[17] P. S. J. Russell, J.-L. Archambault, and L. Reekie, "Fibre gratings," *Physics World*, vol. 6, no. 10, pp. 41–48, 1993.

[18] R. Mahakud, O. Prakash, S. K. Dixit, and J. K. Mittal, "Analysis on the laser beam pointing instability induced fringe shift and contrast dilution from different interferometers used for writing fiber Bragg grating," *Opt. Commun.*, vol. 282, no. 11, pp. 2204–2211, 2009.

[19] R. Mahakud, O. Prakash, J. Kumar, S. V. Nakhe, and S. K. Dixit, "Analysis on the effect of UV beam intensity profile on the refractive index modulation in phase mask based fiber Bragg grating writing," *Opt. Commun.*, vol. 285, pp. 5351–5358, 2012.

[20] S. Antipov, M. Amos, R. J. Williams, E. Magi, M. J. Withford, and A. Fuerbach, "Direct infrared femtosecond laser inscription of chirped fiber Bragg gratings," *Opt. Express*, vol. 24, no. 1, p. 30, 2016.

[21] M. Becker, J. Bergmann, S. Brückner, M. Franke, E. Lindner, M. W. Rothhardt, and H. Bartelt, "Fiber Bragg grating inscription combining DUV subpicosecond laser pulses and two-beam interferometry," *Opt. Express*, vol. 16, no. 23, p. 19169, 2008.

[22] M. Becker, T. Elsmann, A. Schwuchow, M. Rothhardt, S. Dochow, and H. Bartelt, "Fiber Bragg gratings in the visible spectral range with ultraviolet femtosecond laser inscription," *IEEE Photon. Technol. Lett.*, vol. 26, no. 16, pp. 1653–1656, 2014.

[23] A. Othonos, "Fiber Bragg gratings," *Rev. Sci. Instrum.*, vol. 68, no. 12, pp. 4309–4341, 1997.

[24] M. Becker, S. Brückner, M. Leich, E. Lindner, M. Rothhardt, S. Unger, S. Jetschke, and H. Bartelt, "Towards a monolithic fiber laser with deep UV femtosecond-induced fiber Bragg gratings," *Opt. Commun.*, vol. 284, no. 24, pp. 5770–5773, 2011.

[25] J. Skaar, L. Wang, and T. Erdogan, "On the synthesis of fiber Bragg gratings by layer peeling," *IEEE J. Quantum Electron.*, vol. 37, no. 2, pp. 165–173, 2001.
[26] E. Brinkmeyer, "Simple algorithm for reconstructing fiber gratings from reflectometric data," *Opt. Lett.*, vol. 20, no. 8, p. 810, 1995.
[27] D. Keck and R. Modavis, "Low reflectivity fiber Bragg grating with rectangular reflection function," US Patent US005 668 901A, 1997.
[28] M. C. Wu, R. S. Rogowski, and K. K. Tedjojuwono, "Fabrication of extremely short length fiber Bragg gratings for sensor applications," *Proceedings of IEEE Sensors*, vol. 1, no. 1, pp. 49–55, 2002.
[29] Z. Wang, M. Han, F. Shen, and A. Wang, "Ultra-short fiber Bragg grating intrinsic Fabry-Perot interferometric sensors for quasi-distributed strain and temperature sensing," in *SPIE Smart Structures and Materials + Nondestructive Evaluation andHealth Monitoring*, 2007, p. 652935.
[30] J. L. Cruz, L. Dong, S. Barcelos, and L. Reekie, "Fiber Bragg gratings with various chirp profiles made in etched tapers," *Appl. Opt.*, vol. 35, no. 34, pp. 6781–6787, 1996.